White and Grey Matter Abnormalities in Autism Align with Verbal Ability

Sabine V. Huemer[1,*], Frithjof Kruggel[2], Virginia Mann[1] and J.G. Gehricke[3]

[1]*Department of Cognitive Sciences, University of California, Irvine, CA 92697, USA*

[2]*Department of Medical Bioengineering, University of California, Irvine, CA 92697, USA*

[3]*Department of Pediatrics, University of California, Irvine, CA 92697, USA*

Abstract: This whole-brain structural magnetic resonance imaging (MRI) investigation of autism spectrum disorder (ASD) analyzed white and grey matter concentrations, shape differences, and brain microstructure in 20 adolescents with ASD and 10 neurotypical controls. Evidence for significant group-related differences was found in nine regions, most associated with language processing, including the precentral gyrus, the anterior cingulate, the operculum, superior frontal, and superior temporal gyri. An additional analysis revealed that lower scores from a standardized measure of receptive verbal ability correlated with reduced white matter in the arcuate and uncinate fascicles, inthalamo-frontal and thalamo-cerebellar connections, and in interhemispheric connections passing through the callosal sections I and V. Our findings point to distinct neurological subgroups in ASD which align with the level of verbal ability.

Keywords: Autism spectrum disorder, Receptive verbal ability, Neurological subgroups, Adolescents, Structural magnetic resonance imaging.

INTRODUCTION

Autism spectrum disorder (ASD) is a neurodevelopmental disorder characterized by persistent social communication and interaction deficits, and restrictive, repetitive patterns of behavior including intense preoccupations and inflexible adherence to routines. ASD may occur with or without accompanying intellectual impairment and the severity of the disorder may fluctuate over time [1]. In particular, ASD subjects may vary in the extent of verbal impairment, and the potential anatomical correlates of this are a concern of this paper along with the general profile of white and gray matter anomalies associated with ASD.

Several brain regions have been implicated consistently in ASD but results often differ on whether there are increased or decreased brain volumes and whether differences can be found at all in certain regions. The discrepancies may result from differences in imaging protocols, data analysis, subject ages, and samples sizes, but the overall in homogeneity of ASD samples, which disregard neurological and diagnostic subtypes, may play a bigger role than generally assumed. For example, an early magnetic resonance imaging (MRI) study reported decreased volume of the cerebellar vermian lobules VI and VII [2], which are implicated in language, emotion, and executive function

[3], but subsequent studies could not replicate these findings [4]. It is noteworthy that Courchesne *et al*. (1988) worked with a low-functioning autism population, where Piven *et al*. (1992) and Holttum *et al*. (1992) examined high-functioning ASD subjects [2, 4-5]. Other studies have implicated volumetric differences in the frontal lobes in autism [6-7] as well as in the parietal lobes [8] with varying results.

Similar to anatomical results, diffusion tensor imaging (DTI) studies report differing results of increased or decreased white matter, or, no differences between controls and ASD subjects in various brain regions. Brain regions commonly implicated are the corpus callosum [9-13], the cingulate gyrus [13-14], especially the anterior cingulate [12, 15-16], the superior temporal gyrus [17], and the frontallobe [18]. An increasing number of DTI studies point to an aberrant white matter in long-distance neural connections. Significantly lower fractional anisotropy (FA) was found in the uncinate fasciculus of children and adults with ASD [12, 19-21]. White matter abnormalities are also seenin the superior longitudinal fasciculus (SLF) [12-13, 15, 22-23] and one of its parts, the arcuate fasciculus [12, 21], the latter is a major pathway between the language areas of the brain. More recent studies find that in ASD, most or all major neural networks are impaired, rather than isolated, discrete brain regions [13, 24-25]. It is speculated that white matter pathways in higher-order social and cognitive neural circuits are affected most [26].

*Address correspondence to this author at the Loyola Marymount University, Department of Psychology, 1 LMU Dr. Los Angeles CA 900245;
Tel: (310) 245-6041; E-mail: shuemer@lmu.edu

Some studies examined structural abnormalities in relation to functional impairments. Increased amygdala volumes were associated with social and communication deficits [27-28]. DTI studies correlated white matter findings with scores on the commonly used diagnostic tool, Autism Diagnostic Interview – Revised (ADI-R). Cheung *et al*. (2009) reported a tight correlation between lower fractional anisotropy (FA) and higher ADI-R scores, which tied lower FA to a more severe diagnosis of the ASD [22]. Cheung found a correlation between communication and reciprocity impairments and lower FA throughout fronto-stratial-temporal pathways, while repetitive behaviors were correlated with white matter indices in posterior brain pathways, including the splenum of the corpus callosum and cerebellum. Several other studies have correlated scores on the ADI-R and the Childhood Autism Rating Scale (CARS) to white matter abnormalities in ASD and have found correlations between lower FA and more severe forms of ASD [10]. Alexander *et al*. (2007) examined white matter abnormalities in the corpus callosum in ASD children, adolescents, and adults with ASD and found a correlation between lower performance on the IQ measure, the Wechsler Intelligence Scales, and smaller corpus callosum volumes [9]. These findings point to neurologically distinct subgroups in ASD that align with specific abilities or impairments.

In the present study we pursue this indication as we evaluate the relation between our MRI and DTI measures and subjects' performance on the *Peabody Picture Vocabulary Test - Third Addition* [35] (PPVT-III), a test of receptive verbal function. Our previous behavioral work with the PPVT and measures of reading ability have implicated distinct subgroups in which higher-functioning ASD individuals are more closely aligned with controls than with lower-functioning individuals [33]. We seek an anatomical correlate of this in the present study.

Our choice of subjects is adolescents, given the potential role of maturational factors in studies of ASD. Age may be an important factor in the neurodevelopment in ASD. In typical adolescence, a maturation of the structure and myelination of fiber tracts is observed, which is reflected in increasing fractional anisotropy (FA) and decreasing mean diffusivity (MD) and plays a vital role in the cognitive development of the individual [30-31]. Impaired maturation in ASD, for either FA or MD, was reported by several studies [9, 13]. As opposed to evidence showing a trend of lower FA in adolescence, Cheng *et*

al. (2010) found numerous fiber tracts with greater FA in adolescents with ASD and only a few areas of decreased FA, which may again be a reflection of inhomogeneous samples [22].

In the present study, we used structural MRI and DTI to present a detailed analysis of the brain structure of 30 adolescents (20 with ASD and 10 controls) in which we consider not only the diagnosis of ASD but also performance on a test of receptive language as an independent variable in the anatomical analysis. This provides us with a means of examining whether higher order functioning in ASD exhibits a neuroanatomical signature in either degree or location of impairment. Receptive language correlates with the integrity of Wernicke's area of the posterior superior temporal gyrus (STG) and surrounding areas as well as regions involved in speech motor processing [32] and we speculate that we will find anatomical differences in these areas. We also predict that higher-functioning ASD participants will more closely align with controls, consistent with our earlier work on reading and receptive vocabulary [33]. We also expected to find evidence for possible neuroanatomical subtypes in ASD when using verbal ability scores from the PPVT-III as group designation instead of diagnosis.

MATERIALS AND METHODS

Subjects

Twenty participants (ages 12 – 20 years, 5 females, 15 males) with a previous diagnosis of an autism spectrum disorder and 10 typically developing control subjects (ages 12 - 18 years, 1 female, 9 male) were prescreened over the phone and enrolled in our study. Adolescent subjects gave informed written assent in addition to their parent's informed written consent. Adult participants gave informed written consent to the protocol approved by the Internal Review Board at the University of California, Irvine. ASD participants were recruited from local treatment centers, a local autism walk, both ASD and control subjects were also recruited and through word-of-mouth. Seven ASD participants were medicated for one or more common ASD co-morbidities: two for Obsessive Compulsive Disorder (OCD), five for Generalized Anxiety Disorder (GAD), five for Major Depressive Disorder (MDD), three for Attention-Deficit Hyperactivity Disorder (ADHD), one for Tourette Syndrome, and one for synesthesia.

Individuals with braces, electronic or metal devices in or on their body, epilepsy, a history of head injuries, and other severe medical conditions were excluded. In

addition, participants with mental disorders other than ASD were excluded in the ASD group. In the control group, individuals with a reported family history of ASD or any other psychiatric disorders were excluded.

An autism diagnosis was confirmed or rejected, and other psychiatric disorders rejected using *the Schedule for Affective Disorders and Schizophrenia for School-Age Children-Present and Lifetime version, K-SADS-PL* [34], which included an autism module. The K-SADS-PL is a frequently used semi-structured diagnostic interview designed to assess current and past episodes of psychopathology in children and adolescents according to the *Diagnostic and Statistical Manual Fourth Edition* (DSM-IV) criteria. An ASD diagnosis was confirmed by using the criteria from the updated *Diagnostic and Statistical Manual Fifth Edition*, the DSM-5 [1]. All psychological assessments were conducted by the lead investigator under the supervision of a board-certified clinical psychologist. Imaging sessions were conducted by the lead investigator and a trained MRI operator.

Cognitive Assessment

After the initial screening for eligibility and the completion of the psychological assessment, the *Peabody Picture Vocabulary Test Third Addition (PPVT-III)* [35] was administered to all participants by the lead investigator, who has extensive experience administering this test to both ASD and control subjects. The PPVT-III is a wide-range measure of receptive oral vocabulary in Standard English and a screening test for verbal ability, and may as such be seen as a global measure for cognitive functioning [35-36]. Individuals are asked to look at a choice of four simple black-ink drawings per page and select the picture that best matches an aurally presented word. Participants can point to the picture or name the number index of the chosen picture which makes the test more suitable ASD individuals who may prefer to communicate nonverbally. ASD children and adolescents with a previous diagnosis of Asperger Syndrome have shown to achieve scores as high, or higher, than typically developing controls in our prior research study [33]. All participants in the current study completed the cognitive assessment within ten to twenty minutes.

Imaging data acquisition

T_1-weighted MR images were acquired on a Philips Achieva 3T scanner, equipped with an 8-channel phased array coil, using a TFE sequence with TR 11 ms, TE 3.7 ms, flip angle 18 degrees, 150 sagittal slices with a matrix of 240 x 240 voxels, corresponding to an isotropic resolution of 1.0 mm. Diffusion-weighted images were acquired on the same scanner and coil, using a diffusion-weighted spin-echo sequence with TR 7.0 s, TE 80.0 ms, flip angle 90 degrees, 60 axial slices with a matrix of 144 x 144 voxels, corresponding to a resolution of 1.67 x 1.67 mm (in plane), 2 mm slice thickness, 48 gradient directions at b = 1000 s/mm^2, one gradient-free acquisition, and one acquisition with isotropic gradients at b = 0 s/mm^2. Note that at an angulation of 30 degrees w.r.t., the AC-PC plane, not the full intracranial space is imaged: approximately 2 cm of the superior frontal lobe and 4 cm of the posterior cerebellum are cut off. Besides the images, the following variables were collected: group label (GRP, C = control, A = study group), gender (GEN, M = male, F = female), and age at time of examination (AGE, in years).

Imaging data processing and analysis

T_1 weighted scan data in Philips PARREC format were converted into BRIAN format, aligned with the stereotactical coordinate system [37] and interpolated to an isotropical voxel size of 1mm using a fourth-order b-spline method. All datasets were registered with the ICBM 2009c template [38] using a recent approach for nonlinear registration [39]. All registered head images were averaged, correcting for the mean intensity. The brain was extracted from the average to yield the brain template 1. Data were segmented by a fuzzy approach using 3 classes [40], yielding a set of 3 probability images: 0: cerebrospinal fluid, CSF, 1: grey matter, GM, or 2: white matter, WM. As result, gross compartment volumes (in ml) for GM, WM, CSF, and intracranial volume (ICV) were obtained for all subjects (method AAL). All intensity-corrected brain images were registered with template 1, and averaged to yield the brain template 2. The resulting GM probability map in MNI space was divided into regions-of-interests (ROIs) using the AAL template [41]. This analysis yielded GM concentrations in 116 ROIs. Linear regression models were computed for each ROI, using the GM concentration as a dependent variable, and variables group (GRP), age (AGE), and gender (GEN) as independent variables. Data were smoothed using a Gaussian filter (σ = 2, FWHM of 4.7 mm), and log-transformed. Linear regression models were computed for each voxel, using log (JAC) as a dependent variable, and variables GRP, AGE, GEN, and intracranial volume (ICV) as independent variables. As

result, the significance of the group-related shape differences, expressed as voxel-wise z-scores were obtained. This technique is commonly denoted as tensor-based morphometry (TBM) [42] (method TBM).

GM and WM concentrations warped into in MNI space were smoothed using a Gaussian filter (σ = 2, FWHM of 4.7 mm) and log it-transformed. Linear regression models were computed for each voxel, using the transformed concentration as a dependent variable, and variables GRP, AGE, GEN, and ICV as independent variables. Computation was restricted to a GM (WM) mask with a GM (WM) probability $p > 0.25$. As result, the significance of the group-related GM (WM) differences, expressed as voxel-wise z-scores were obtained. Note that negative (positive) z-scores correspond to a locally lower (higher) GM or WM concentration of study subjects vs. controls. This technique is commonly denoted as voxel-based morphometry (VBM) [43] (method VBM-GM and VBM-WM).

For TBM and VBM, clusters above an absolute z-score threshold of 2.5 were determined and addressed a significance based on the theory of excursion sets in Gaussian random fields according to Friston and Worsley [44].

Diffusion tensors were computed from the registered diffusion-weighted images using a nonlinear procedure including anisotropic noise filtering [47]. Tensors were converted into fractional anisotropy (FA), mean diffusivity (MD), and radial diffusivity (RD) values. Note that negative (positive) z-scores correspond to a locally lower (higher) directness of WM fibers of study subjects vs. controls (method DTI-FA, DTI-MD, DTI-RD).

Statistical Analysis

Global and regional volumetric measures were assessed with AGE, GEN, and GRP as independent variables. Age and gender are balanced across group designation, so interaction terms do not have to be incorporated. Variables ICV, GMV, WMV, and CSFV do not depend on AGE, GEN, and GRP. Next, compartment volumes were normalized by the intracranial volume. GMR and WMR showed a significant dependence on AGE only: for GMR: -0.5593 %/year, for WMR+0.3568 %/year. CSFR was independent of all variables. Next, the dependence of the GM concentrations in all regions of the AAL template was analyzed and results were compiled in Table **1**.

For a combined evaluation, results of the three voxel-based analyses (VBM-GM, VBM- WM, TBM) were mapped together in MNI space, and overlaid onto template 2. Method DTI did not result in any significant findings. Leaving out the motion-disturbed data of ASD subjects 7 and 9, and control subject 8 slightly improved results. Results are compiled in Table **2** and Figures **1**-**7**.

As an alternative to the analysis by group designation, the results of the Peabody Picture Vocabulary Test Third Edition (PPVT-III) were used as the independent variable in the anatomical analysis. Note that the correlation between the group designation and the PPVT-III is not significant (*p=0.12*).

Table 1: Regions of Significant Differences of GMC as Revealed by AAL Analysis

#	Method	Structure	Δ%	p-value
1	AAL	Mid Frontal Gyrus L (orb)	-0.0341	0.024
2	AAL	Sup Frontal Gyrus L (orb)	-0.0301	0.007
3	AAL	Mid Frontal Gyrus L	-0.0235	0.047
4	AAL	Inf Frontal Gyrus L (oper)	-0.0274	0.049
5	AAL	Olfactory Gyrus L	-0.0686	0.011
6	AAL	Lingual Gyrus R	-0.0373	0.005
7	AAL	Fusiform Gyrus R	-0.0306	0.011
8	AAL	Mid Temporal Gyrus L	-0.0179	0.036
9	AAL	Sup Temporal Gyrus R	-0.0235	0.025
10	AAL	Inf Temporal Gyrus R	-0.0249	0.04

Notes: All ROIs show a lower GMC in subjects with ASD.

Table 2: Significant Results from VBM-GM, VBM-WM, and TBM for the ASD Group

#	Method	Structure	Coordinates			Size	z_{max}	z_{av}
			x	**y**	**z**	**mm³**		
11	GM	Mid Frontal Gyrus L	-34	48	25	928	-3.379	-2.319
12	GM	Inf Frontal Gyrus L	-40	21	-7	808	-4.027	-2.490
13	GM	Med Frontal Gyrus L	-4	28	-13	1370	-3.244	-2.340
14	GM	Inf Temporal Gyrus L	-40	-11	-32	911	-2.998	-2.258
15	GM	Mid Frontal Gyrus R	36	9	39	1116	-3.261	-2.412
16	GM	Sup Temporal Gyrus R	48	-19	-1	1674	-4.177	-2.549
17	WM	Frontal Lobe WM L	36	-33	39	986	2.982	2.357
18	WM	Frontal Lobe WM R	32	8	37	1756	3.425	2.483
19	WM	Mid Frontal Gyrus WM L	-36	11	37	951	3.132	2.287
20	WM	Mid Temporal Gyrus WM R	47	-45	8	932	3.778	2.405
21	WM	Sup Temporal Gyrus WM R	48	-23	-2	1637	4.102	2.634
22	WM	Postcentral Gyrus WM R	46	-20	52	942	-4.071	-2.386
23	WM	Cingulate Gyrus WM L	-17	-21	49	787	-3.389	-2.353
24	WM	Frontal Lobe Sub-Gyral WM R	22	24	29	1125	-3.191	-2.341
25	TBM	Paracentral Lobule WM R	10	-27	53	1253	3.457	2.846
26	TBM	Sub-lobar Extra-Nuclear WM R	31	-3	-11	3417	4.391	3.016
27	TBM	Sub-lobar Extra-Nuclear WM L	-34	3	-8	1018	2.867	2.284
28	TBM	Sup Frontal Gyrus WM L	-23	34	41	3263	-4.616	-2.909
29	TBM	Sup Frontal Gyrus GM R	30	46	29	376	-3.247	-2.733
30	TBM	Sub-lobar Extra-Nuclear WM R	2	-21	11	648	-3.051	-2.674
31	TBM	Inf Temporal Gyrus L	-50	-42	-17	1922	-3.460	-2.759

Notes: The sign of the z-scores is given relative to typically developing controls. Leaving out the motion-disturbed data of ASD subjects S07 & S09 and control C08 slightly improved results.

Also note that a positive correlation of anatomical findings with the PPVT-III should be interpreted as a "more normal" finding. Percentile results of the PPVT-III Standard Scores were used here. Results can be viewed in Figures **8** and **9**.

To examine how much this reduced maturation can be found in other WM regions, even if sub-threshold, all statistics were recomputed without a threshold, and combined so that effects add up, *e.g*., $z_{WM} + z_{FA} - z_{MD} - z_{RD}$. Thus, higher z-scores correspond to a lower content of extra-cellular space, or higher white matter maturation. No attempt was made to apply weighting (or correction) factors to this statistic. Results can be seen in Figure **10**.

RESULTS

Evidence for ASD vs control group-related differences was found for nine regions, compiled in Figures **1** and **7**. Reduced white matter maturation is found to correlate with lower PPVT-III scores, most prominently in the arcuate and uncinate fascicles (L and R), in thalamo-frontal and thalamo-cerebellar connections, and in interhemispheric connections passing through the callosal sections I and V, regardless of group designation.

Grey Matter Concentration Differences

The ASD group showed a significantly lower grey matter concentration (GMC) in inferior portions of the left frontal lobe, most notably the operculum, which includes Brodmann area 44 (BM44), and the left inferior temporal gyrus. Homologue regions were also found in the right frontal lobe, but did not reach statistical significance (see Figure **1**). Lower GMC was also found in the medial frontal gyrus on the left, specifically in the anterior cingulate. AAL regions 1-5 (see Table **1**) correspond to grey matter regions ROI 11 -15 (see Table **2**). We also found lower GMC in the
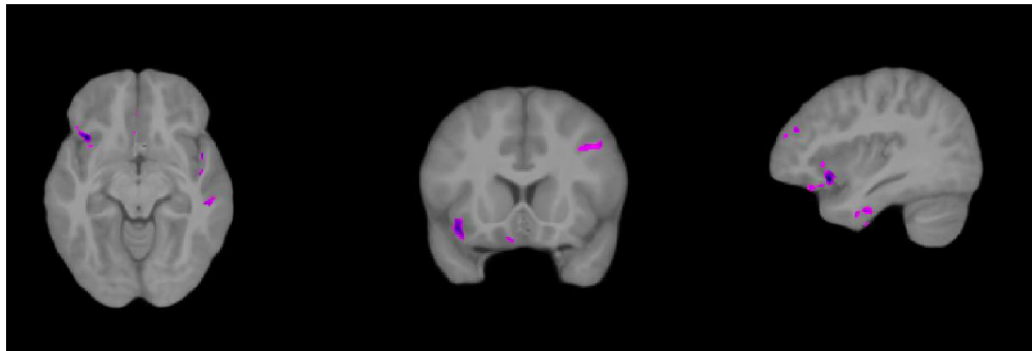
Figure 1 : Group-related differences in GMC in left frontal lobe.
Note: Regions of lower GMC in ASD children is found in inferior portions of the left frontal lobe, most notably, in the frontal operculum. Homologue regions were also found in the right frontal lobe, but did not reach statistical significance. AAL regions 1-5 correspond to GM regions 11, 12, 13, and 15.
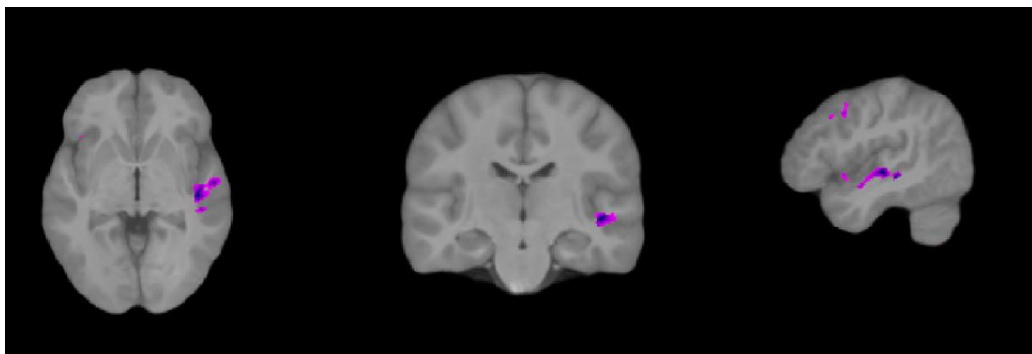
Figure 2: Group-related differences in GMC in right STG.
Note: A region of lower GMC in ASD children is found in the right superior temporal gyrus. Region 9 (AAL) and 15, 16 (VBM-GM) correspond.
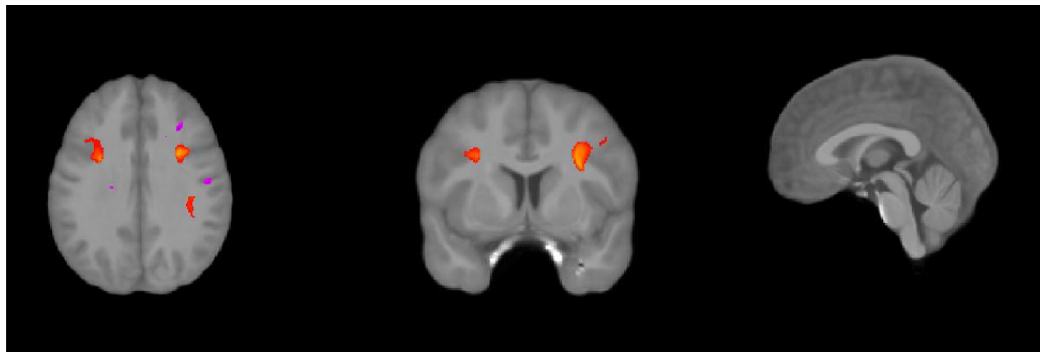
Figure 3: Group-related differences in WMC in frontal lobes.
Note: A region of higher WMC is found in the upper portions of the frontal lobe on both sides (ROIs 19, 20).

ASD group in the right superior temporal gyrus and the right precentral gyrus. (see Figure **2**). ROI 9 (AAL) and 15, 16 (VBM-GM) correspond.

White Matter Concentration Differences

Adolescents with ASD showed a significantly higher white matter concentration (WMC) in the upper portions of the frontal lobe on both sides, specifically the left and right precentral gyrus. More increases in WMC were found in the middle temporal gyrus and the superior temporal gyrus on the right. ROIs 17, 18, 19, and 20 correspond (see Figure **3**). Significantly lower WMC in the ASD group was found in the right postcentral gyrus, an area that receives the bulk of thalamocortical projections from sensory input fields. Lower WMC in the ASD group was also found in the mid portions of the right frontal lobe and the left cingulate gyrus. ROIs 22, 23, and 24 correspond.

Shape Differences

Group-related shape differences included a region of significant shrinkage in the ASD group in the superior portions of the white matter in the left frontal lobe, specifically the left middle frontal gyrus (ROI 28), less prominent on the right superior frontal gyrus (ROI 29) (see Figure **5**). A region of significant expansion

was found in anterior portions of the white matter stalk of the superior temporal gyrus and external capsule on both sides, including the right and left claustrum. These regions are in over-projection with the uncinate fasciculus (ROIs 26 and 27) (see Figure **5**). A region of significant shrinkage in the ASD group was exposed along the inferior temporal gyrus and the fusiform gyrus on the left side (ROI 31) (see Figure **7**).
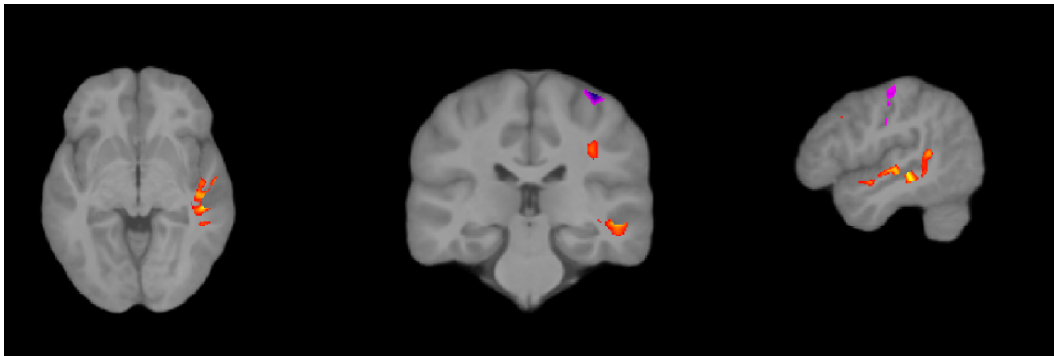
Figure 4: Group-related differences in WMC in STG and MTG.
Note: A region of higher WMC is found in the right superior (and medial) temporal gyrus (ROIs 20, 21).
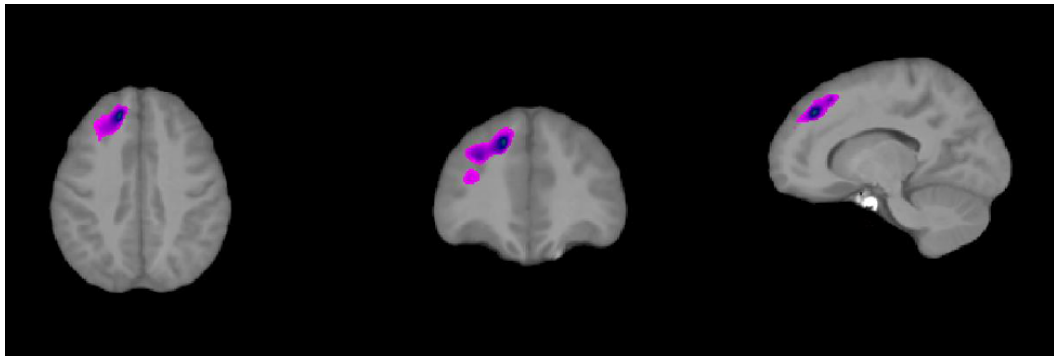
Figure 5: Group-related shape differences as detected by TBM in frontal lobe.
Note: A region of a significant shrinkage is found in the superior portions of the white matter in the left frontal lobe (ROI 28), less prominent on the right side (ROI 29).
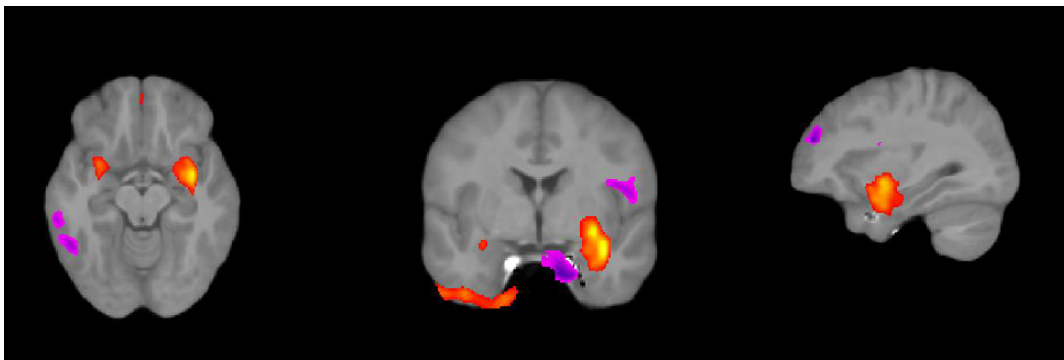
Figure 6: Group-related shape differences as detected by TBM in STG.
Note: A region of a significant expansion is found in anterior portions of the white matter stalk of the superior temporal gyrus and external capsule on both sides. These regions are in over-projection with the uncinate fascicle (ROI 26, 27).
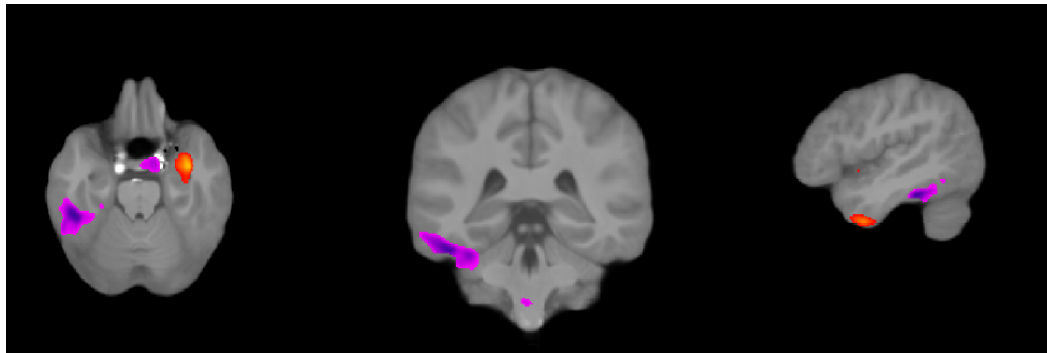
Figure 7: Group-related shape differences as detected by TBM in IFG and fusiform gyrus.
Note: A region of a significant shrinkage is found along the inferior temporal gyrus and fusiform gyrus on the left side (ROI 31).

PPVT-III Scores as Independent Variable

Significantly increased GMC in the parahippocampal gyrus, along with an increased WMC and increased FA in the adjacent white matter of the temporal lobe were correlated with lower PPVT scores (see Figure **8**). Several regions with increased white matter density, increased FA, and decreased medial and radial diffusivity (MD and RD) were found in the lower scoring subjects. Towards the ASD subjects, this is interpreted as a higher regional content of extra-cellular space, or a reduced maturation of local white matter. Such regions are found in the frontal white matter of both hemispheres, along the arcuate fasciculus, L and R, and uncinate fasciculus, L (see Figure **9**).
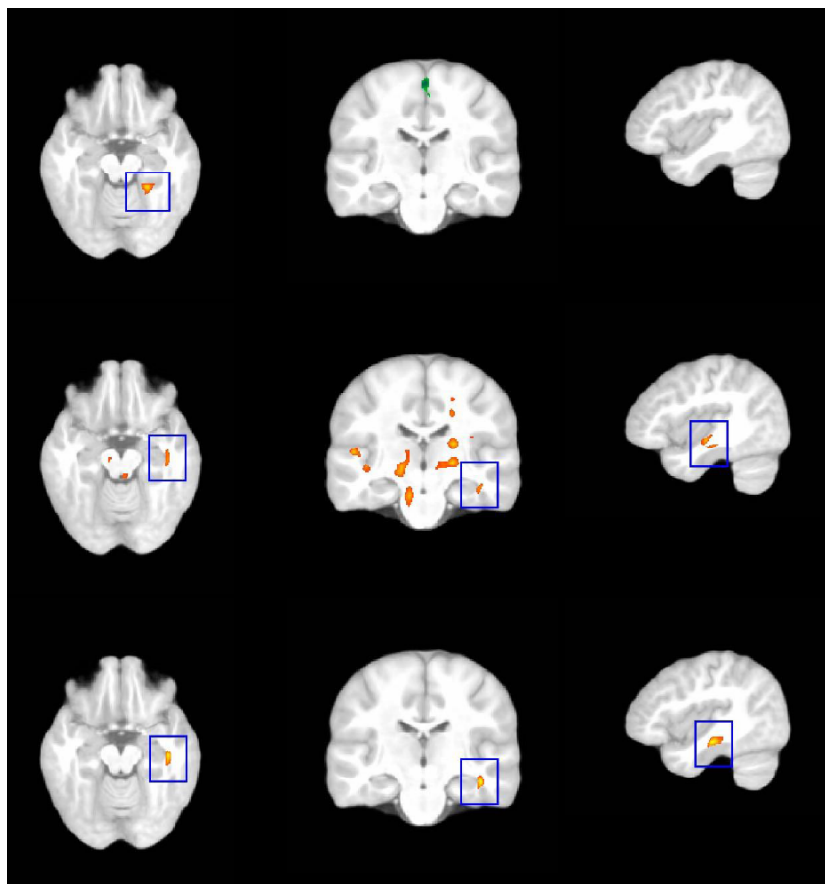
Figure 8: PPVT-related differences in parahippocampal gyrus and temporal lobes.
Note: PPVT-related differences in grey matter concentration (GMC, top), white matter concentration (WMC, middle), and fractional anisotropy (FA, below). A region of increased GMC is found in the parahippocampal gyrus, along with an increased WMC and increased FA in the adjacent WM of the temporal lobe.
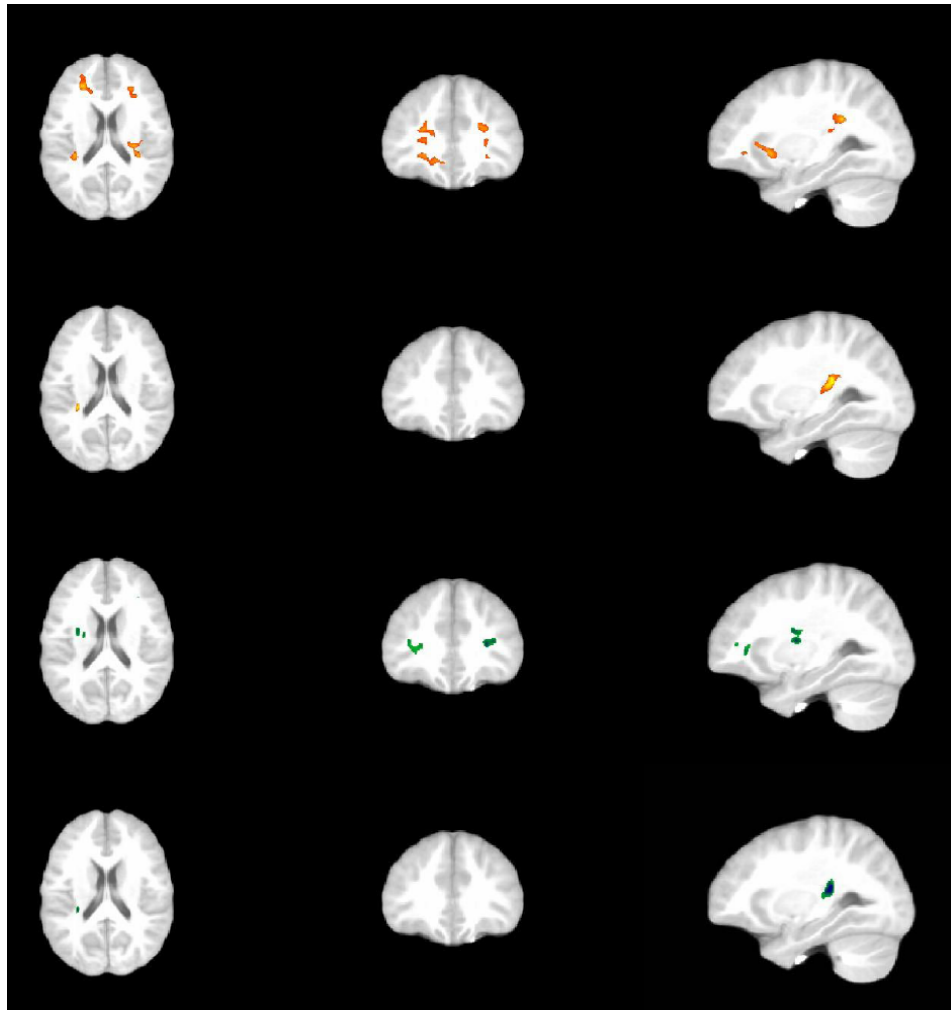
Figure 9: PPVT-related differences in frontal lobes along AF and UF.

Note: PPVT-related differences in white matter concentration (WMC, top), fractional anisotropy (FA, 2nd row), mean diffusivity (MD, 3rd row), and radial diffusivity (RD, be- low). Several regions with increased WM density, increased FA, and decreased MD and RD were found. Towards the ASD subjects, this is interpreted as a higher regional content of extra-cellular space, or a reduced maturation of local WM. Such regions are found in the frontal WM of both hemispheres, along the arcuate fascicle (L and R), and uncinate fascicle (L).

SUMMARY STATISTICS

The results indicate increased maturation of white matter bundles of the arcuate fasciculus (top left), in the frontal white matter adjacent to the frontal eye field (top right), and the uncinate fascicles on both sides (below) (see Figure **10**). Further summary statistics revealed the increased maturation of white matter bundles in the anterior section of the corpus callosum (I), the posterior section (V), and thalamo-frontal connections on both sides (top right), and the thalamo-cerebellar connections (see Figure **10**).

DISCUSSION AND CONCLUSION

As expected, our findings show overlapping areas of anomalies in grey and white matter concentrations in the frontal and temporal lobes and in long-distance association and projection fibers in the ASD group, often in areas instrumental in language processing. Volumetric and shape differences were found in areas known to mediate receptive verbal ability, and these correlated with the PPVT measure. Interestingly, when the continuous PPVT measure replaced diagnostic groups as a variable, the results indicate that the neurological profile of high functioning ASD subjects lies on a continuum with typically developing controls rather than clustering with that of ASD subjects with more severe cognitive impairments. This implies that individuals on the high-functioning side of the ASD spectrum, who typically are individuals with higher verbal skills, are neurologically more like typically developing teens than their peers on the lower-functioning end of the ASD spectrum, who have lower verbal skills.
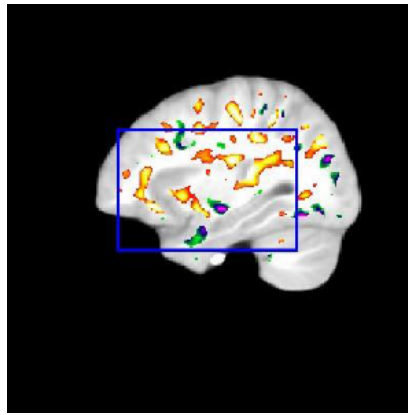
Note: Increased maturation of WM bundles of the arcuate fascicle
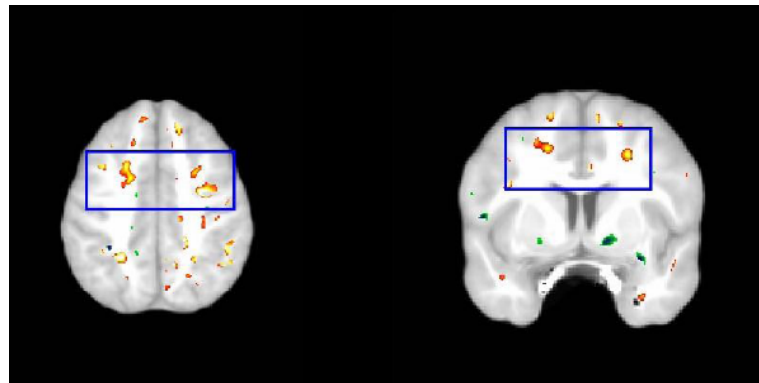
Note: Increased maturation of WM bundles in the frontal WM adjacent to the frontal eye field
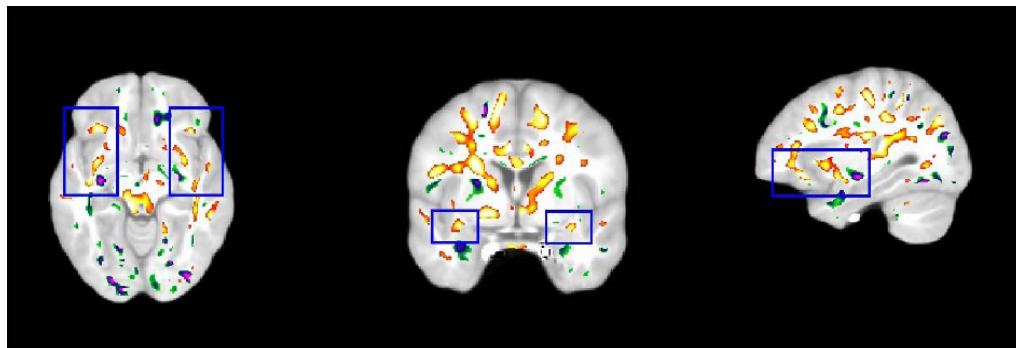
Note: Increased maturation of WM bundles in the uncinate fascicle on both sides

Figure 10: PPVT Summary Statistics.

Below, we summarize the results of our study as compared to previous research, specifically the anatomical correlates that associate with verbal ability.

White and Grey Matter Abnormalities in ASD

Our initial analysis revealed significantly lower grey matter concentration in the ASD group in the left frontal lobe and the left inferior temporal gyrus, including Broca's (BA44), an area instrumental in language production and comprehension. McAlonan *et al*. (2008) found a significant negative correlation between the

size of a grey matter cluster around BA44 and the onset of speech in high-functioning children with autism [29]. Other prior DTI research presents evidence of white matter abnormalities in frontal lobe regions involved in verbal ability. For example, Sundaram *et al*. (2008) found less FA in short range fibers and more FA in long range association fibers in the frontal lobe in ASD [18]. Cheung *et al*. (2009) found lower FA in the left and right prefrontal and temporal regions [22].

We also found lower grey matter concentrations alongside increased white matter concentrations in the

ASD group in the right superior temporal gyrus (STG). Bigler *et al*. (2007) found no volumetric STG differences between groups, but a positive correlation between left STG size and receptive verbal abilities and IQ scores in controls while the ASD group showed no correlation [46]. This supports the relationship between receptive verbal ability and white matter volumes in the STG. In the present study we found that reduced vocabulary associated with increased grey matter concentration in the parahippocampal gyrus, along with an increased white matter concentration and increased FA in the adjacent white matter region of the temporal lobe that aligned with scores from the PPVT-III. Our analysis also revealed a region of significant expansion in anterior portions of the white matter stalk of the STG.

White Matter Abnormalities Align with Receptive Verbal Ability

When we used PPVT scores instead of group designation, we found several regions with increased white matter density, increased FA, and decreased MD and RD in the lower scoring subjects including both sides of the arcuate fasciculus and the left uncinate fasciculus (see Results section under *PPVT scores as independent variable*). The arcuate fasciculus is part of the superior longitudinal fasciculus and connects parts of the temporal and parietal lobe bidirectionally with the frontal lobe, specifically, it is said to connect Broca's area with Wernicke's area, two areas instrumental in language production and processing. White matter abnormalities were previously found in the superior longitudinal fasciculus, a bi-directional long-distance association fiber bundle, which connects the frontal, temporal, occipital, and parietal lobes [12-13, 22-23]. The superior longitudinal fasciculus consists of four distinct components which operate independently, one of them is the arcuate fasciculus which also has shown specific neuroanatomical and functional abnormalities in ASD [12, 21].

Limitations

One of the limitations of our study was sample size. While we had well-matched controls and a good balance of age, gender, and cognitive levels, age had effects on our results, therefore a different sample may yield different results. Another possible limit may be medication. Our sample included 7 ASD participants who were medicated for symptoms from co-morbid disorders that are commonly found alongside ASD. We decided to include these individuals for numerous reasons, (i) a fully non-medicated sample may be

biased toward ASD individuals on the mild side of the spectrum, (ii) many ASD adolescents have been medicated at some point in their development, (iii) medication alleviates behaviors derived from comorbidities and may reveal the "true nature" of ASD in the individual, and (iv) we do not know the effects of medication on brain growth and structure. Previous DTI studies with ASD populations have found no correlation between psychotropic medications and outcomes [17]. Comorbidities are often part of ASD, they are frequently difficult to discern from the primary diagnosis, and often go undiagnosed and unreported. Therefore, an exclusion may lead to samples that do not adequately represent the heterogeneity of the disorder.

CONCLUSION

Our results reveal significant white and grey matter abnormalities in ASD, specifically in regions associated with language processing. We found that ASD individuals with higher receptive verbal ability scores are neurologically more similar to controls than they are to lower performing individuals, and that white matter anomalies in long distance and language pathways were significantly correlated with lower receptive verbal ability scores. Our findings indicate neurological sub-groups in ASD that align with receptive verbal function. These findings partially overlap with previous research that shows a correlation between lower verbal abilities and IQ and lower corpus callosum volumes [9]. Our results are also reminiscent of studies suggesting neuropathological subgroups within the ASD spectrum [29, 47], which are related to distinct ASD behaviors [10].

Our findings are noteworthy since imaging research in ASD has provided largely inconclusive results due to in homogeneities of study subjects with ASD who lie on a wide spectrum of abilities and impairments. Grouping study subjects by verbal ability may produce clearer future imaging results and help target treatment efforts. Future studies may investigate which neuro-structural abnormalities are specific to ASD and which are purely related to lower cognitive functioning. More research is needed to define neurological profiles that capture the diversity of the ASD spectrum.

contributed the study design and imaging protocol, subject recruitment, assessments and procedures including imaging and imaging processing, and the write up of results. Frithj of Kruggel conducted the statistical analysis. Virginia Mann provided departmental funding and contributed in terms of proofreading and editing. Jean Gehricke supervised the administration of the K-SADS and provided clinical advice and support services.

REFERENCES

[1] American Psychiatric Association. Diagnostic and Statistical Manual of Mental Disorders. Fifth Edition. Arlington, VA, American Psychiatric Association, 2013.

[2] ourchesne E, Yeung-Courchesne R, Press GA, Hesselink JR, Jernigan TL. Hypoplasia of cerebellar vermal lobules VI and VII in autism. N Engl J Med 1988; 318: 1349-1354.
http://dx.doi.org/10.1056/NEJM198805263182102

[3] Hodge SM, Makris N, Kennedy DN, Caviness VS, Howard J, McGrath L *et al*. Cerebellum, language, and cognition in autism and specific language impairment. J Autism Dev Disord 2010; 40: 300-316.
http://dx.doi.org/10.1007/s10803-009-0872-7

[4] Piven J, Nehme E, Simon J, Barta P, Pearlson G, Folstein SE. Magnetic resonance imaging in autism: Measurement of the cerebellum, pons, and fourth ventricle Biol Psychiatry 1992; 31: 491-504.
http://dx.doi.org/10.1016/0006-3223(92)90260-7

[5] Holttum JR, Minshew NJ, Sanders RS, Phillips NE. Magnetic resonance imaging of the posterior fossa in autism. Biol Psychiatry 1992; 32: 1091-1101.
http://dx.doi.org/10.1016/0006-3223(92)90189-7

[6] Carper RA, Courchesne E. Inverse correlation between frontal lobe and cerebellum sizes in children with autism. Brain 2000; 123: 836-44.
http://dx.doi.org/10.1093/brain/123.4.836

[7] Courchesne RY. Unusual brain growth patterns in early life in patients with autistic disorder: An MRI study. Neurology 2001; 57: 245-254.
http://dx.doi.org/10.1212/WNL.57.2.245

[8] Courchesne E, Press GA, Yeung-Courchesne R. Parietal lobe abnormalities detected with MR in patients with infantile autism. AJR Am J Roentgenol 1993; 160: 387-93.
http://dx.doi.org/10.2214/ajr.160.2.8424359

[9] Alexander AL, Lee JE, Lazar M, Boudos R, DuBray MB, Oakes TR *et al*. Diffusion tensor imaging of corpus callosum in autism. Neuroimage 2007; 34: 61-73.
http://dx.doi.org/10.1016/j.neuroimage.2006.08.032

[10] Hong S, Ke X, Tang K, Hang Y, Chu K, Huang H *et al*. Detecting abnormalities of corpus callosum connectivity in autism using magnetic resonance imaging and diffusion tensor tractography. Psychiatry Res 2011; 194: 333-339.
http://dx.doi.org/10.1016/j.pscychresns.2011.03.009

[11] Keller TA, Kana RK, Just MA. A developmental study of the structural integrity of white matter in autism. Neuroreport 2007; 18: 23-27.
http://dx.doi.org/10.1097/01.wnr.0000239965.21685.99

[12] Kumar A, Sundaram SK, Sivaswamy I, Behen ME, Makki MI, Ager J *et al*. Alterations in frontal lobe tracts and corpus callosum in young children with autism spectrum disorder. Cereb Cortex 2010; 20: 2103-2201.
http://dx.doi.org/10.1093/cercor/bhp278

[13] Shukla DK, Keehn B, Mueller RA. Tract-specific analyses of diffusion tensor imaging shows widespread white matter compromise in autism spectrum disorder. J Child Psychol Psychiatry 2011; 52(3): 286-295.
http://dx.doi.org/10.1111/j.1469-7610.2010.02342.x

[14] Cheng Y, Chou KH, Chen IY, Fan YT, Decety J, Lin CP. Atypical development of white matter microstructure in adolescents with autism spectrum disorders. Neuroimage 2010; 50: 873-882.
http://dx.doi.org/10.1016/j.neuroimage.2010.01.011

[15] Barnea-Goraly N, Kwon H, Menon V, Eliez S, Lotspeich L, Reiss AL. White matter structure in autism. Preliminary evidence from diffusion tensor imaging. Biol Psychiatry 2004; 55: 323-326.
http://dx.doi.org/10.1016/j.biopsych.2003.10.022

[16] Thakkar KN, Polli FE, Joseph RM, Tuch DS, Hadjikhani N, Barton JS *et al*. Response monitoring, repetitive behavior and anterior cingulate abnormalities in autism spectrum disorders (ASD) Brain 2008; 131: 2464-2478.
http://dx.doi.org/10.1093/brain/awn099

[17] Lee JE, Bigler ED, Alexander AL, Lazar M, DuBray MB, Chung MK, Lainhart JE. Diffusion tensor imaging of white matter in the superior temporal gyrus and temporal stem in autism Neurosci Lett 2007; 424: 127-132.
http://dx.doi.org/10.1016/j.neulet.2007.07.042

[18] Sundaram SK, Kumar A, Makki MI, Behen ME, Chugani HT, Chugani DC. Diffusion tensor imaging of frontal lobe in autism spectrum disorder Cereb Cortex 2008; 18: 2659-2665.
http://dx.doi.org/10.1093/cercor/bhn031

[19] Cheon KA, Kim YS, Oh SH, Park SY, Yoon HW, Herrington J *et al*. Involvement of the anterior thalamic radiation in boys with high functioning autism spectrum disorders: a diffusion tensor imaging study. Brain Res 2011; 1417: 77-86.
http://dx.doi.org/10.1016/j.brainres.2011.08.020

[20] Pugliese L, Catani M, Ameis S, Dell'Acqua F, Thiebaut de Schotten M, Murphy C *et al*. The anatomy of extended limbic pathways in Asperger syndrome: A preliminary diffusion tensor imaging tractography study. Neuroimage 2009; 47(2): 427-34.
http://dx.doi.org/10.1016/j.neuroimage.2009.05.014

[21] Sahyoun CP, Belliveau JW, Mody M. White-matter integrity and pictorial reasoning in high-functioning children with autism. Brain Cogn 2010; 73: 180-188.
http://dx.doi.org/10.1016/j.bandc.2010.05.002

[22] Cheung C, Chua SE, Cheung V, Khong PL, Tai KS, Wong TK *et al*. White matter fractional anisotropy differences and correlates of diagnostic symptoms in autism. J Child Psychol Psychiatry 2009; 50: 1102-1112.
http://dx.doi.org/10.1111/j.1469-7610.2009.02086.x

[23] Weinstein M, Ben-Sira L, Levy Y, Zachor DA, Ben Itzhak E, Artzi M *et al*. Abnormal white matter integrity in young children with autism. Hum Brain Mapp 2011; 32: 534-543.
http://dx.doi.org/10.1002/hbm.21042

[24] McAlonan GM, Cheung V, Cheung C, Suckling J, Lam GY, Tai KS *et al*. Mapping the brain in autism. A voxel-based MRI study of volumetric differences and intercorrelations in autism. Brain 2005; 128: 286-276.

[25] Mueller RA. The study of autism as a distributed disorder. Ment Retard Dev Disabil Res Rev 2007; 13: 85-95.
http://dx.doi.org/10.1002/mrdd.20141

[26] Ameis SH, Fan J, Rockel C, Voineskos AN, Lobaugh NJ, Soorya L *et al*. Impaired structural connectivity of socio-emotional circuits in autism spectrum disorders: a diffusion tensor imaging study. PLoS One 2011; 6: 28044.
http://dx.doi.org/10.1371/journal.pone.0028044

[27] Schumann CM, Barnes CC, Bloss CS, Lord C, Courchesne E. Amygdala enlargement in toddlers with autism related to severity of social and communication impairments. Biol Psychiatry 2009; 66942-949.
http://dx.doi.org/10.1016/j.biopsych.2009.07.007

[28]   Sparks B, Friedman S, Shaw D, Aylward E, Echeland D, Artru A *et al*. Brain structural abnormalities in young children with autism spectrum disorder. Neurology 2002; 59(2): 184-92.
http://dx.doi.org/10.1212/WNL.59.2.184

[29]   McAlonan GM, Suckling J, Wong N, Cheung V, Lienenkaemper N, Cheung C *et al*. Distinct patterns in grey matter abnormalities in high-functioning autism and Asperger's syndrome. J Child Psychol Psychiatry 2008; 49(12): 1287-1295.
http://dx.doi.org/10.1111/j.1469-7610.2008.01933.x

[30]   Ashtari M, Cervellione KI, Hasan KM, Wu J, McIlree C, Kester C *et al*. White matter development during late adolescence in healthy males: a cross-sectional diffusion tensor imaging study. Neuroimage 2007; 35: 501-510.
http://dx.doi.org/10.1016/j.neuroimage.2006.10.047

[31]   Schmithorst VJ, Wilke M, Dardzinski BJ, Holland SK. Cognitive functions correlate with white matter architecture in a normal pediatric population: a diffusion tensor imaging study. Hum Brain Mapp 2005; 26: 139-147.
http://dx.doi.org/10.1002/hbm.20149

[32]   Edwards E, Nagarajan S, Dalal S, Canolty R, Kirsch H, Barbaro N *et al*. Spatiotemporal imaging of cortical activation during verb generation and picture naming. Neuroimage 2010; 50(1): 291-301.
http://dx.doi.org/10.1016/j.neuroimage.2009.12.035

[33]   Huemer SV, Mann V. A comprehensive profile of decoding and comprehension in autism spectrum disorders. J Autism Dev Disord 2010; 40: 484-493.
http://dx.doi.org/10.1007/s10803-009-0892-3

[34]   Kaufman J. K-SADS-PL. J Am Acad Child Adolesc Psychiatry 2000; 39(10): 1208.
http://dx.doi.org/10.1097/00004583-200010000-00002

[35]   Dunn L, Dunn L. 1997. The Peabody Picture Vocabulary Test–Third Edition. Circle Pines, MN: American Guidance Service.

[36]   Castellino S, Tooze J, Flowers L, Parsons S. The peabody picture vocabulary test as a pre-screening tool for global cognitive functioning in childhood brain tumor survivors. J Neurooncol 2011; 104(2): 559-563.
http://dx.doi.org/10.1007/s11060-010-0521-1

[37]   Kruggel F, von Cramon DY. Alignment of magnetic-resonance brain datasets with the stereo- tactical coordinate system. Med Image Anal 1999; 3: 111.
http://dx.doi.org/10.1016/S1361-8415(99)80005-X

[38]   Fonov VS, Evans AC, McKinstry RC, Almli CR, Collins DL. Unbiased nonlinear average age-appropriate brain templates from birth to adulthood. Neuroimage 2009; 47(1): 102.
http://dx.doi.org/10.1016/S1053-8119(09)70884-5

[39]   Vercauteren T, Pennec X, Perchant A, Ayache N. Diffeomorphic demons: Efficient non- parametric image registration. Neuroimage 2009; 49: 61-72.
http://dx.doi.org/10.1016/j.neuroimage.2008.10.040

[40]   Pham DL, Prince JL. An adaptive fuzzy segmentation algorithm of magnetic resonance images. IEEE Trans Med Imaging 1999; 18: 737-752.
http://dx.doi.org/10.1109/42.802752

[41]   Tzourio-Mazoyer N, Landeau B, Papathanassiou D, Crivello F, Etard O, Delcroix N. Automated anatomical labeling of activations in SPM using a macroscopic anatomical parcellation of the MNI MRI single subject brain. Neuroimage 2002; 15: 273-289.
http://dx.doi.org/10.1006/nimg.2001.0978

[42]   Chung MK, Worsley KJ, Paus T, Cherif C, Collins DL, Giedd JN *et al*. A unified statistical approach to deformation-based morphometry. Neuroimage 2001; 14: 595-606.
http://dx.doi.org/10.1006/nimg.2001.0862

[43]   Fillard P, Pennec X, Arsigny V, Ayache N. Clinical DT-MRI Estimation, Smoothing, and Fiber Tracking With Log-Euclidean Metrics. IEEE Trans Med Imaging 2007; 26: 14761-1482.
http://dx.doi.org/10.1109/TMI.2007.899173

[44]   Ashburner J, and Friston KJ. Voxel-based morphomoetry. The Methods NeuroImage 2000; 11, 805-821.
http://dx.doi.org/10.1006/nimg.2000.0582

[45]   Friston KJ, Worsley KJ, Frackowiak RSJ, Mazziotta JC, and Evans AC. Assessing the significance of focal activations using their spatial extent. Human Brain Mapping 1993; 1: 210-220.
http://dx.doi.org/10.1002/hbm.460010306

[46]   Bigler ED, Mortensen S, Neeley ES, Ozonoff S, Krasny L, Johnson M *et al*. Superior temporal gyrus, language function, and autism. Dev Neuropsychol 2007; 31(2): 217-238.
http://dx.doi.org/10.1080/87565640701190841

[47]   Raznahan A, Toro R, Daley E, Robertson D, Murphy C, Deeley Q *et al*. Cortical anatomy in autism spectrum disorder: an in vivo MRI study on the effect of age. Cereb. Cortex 2010; 20: 1332-1340.
http://dx.doi.org/10.1093/cercor/bhp198